

# Quark mass dependence of $\rho$ and $\sigma$ Mesons from Dispersion Relations and Chiral Perturbation Theory

C. Hanhart<sup>a</sup>, J. R. Peláez<sup>b</sup> and G. Ríos<sup>b</sup>

<sup>a</sup> *Institut für Kernphysik (Theorie), Forschungszentrum Jülich, D-52425 Jülich, Germany and*  
<sup>b</sup> *Dept. Física Teórica II. Universidad Complutense, 28040, Madrid. Spain.*

We use the one-loop Chiral Perturbation Theory  $\pi\pi$ -scattering amplitude and dispersion theory in the form of the inverse amplitude method to study the quark mass dependence of the two lightest resonances of the strong interactions, the  $f_0(600)$  ( $\sigma$ ) and the  $\rho$  meson. As main results we find that the  $\rho\pi\pi$  coupling constant is almost quark mass independent and that the  $\rho$  mass shows a smooth quark-mass dependence while that of the  $\sigma$  shows a strong nonanalyticity. These findings are important for studies of the meson spectrum on the lattice.

PACS numbers:

Although studied theoretically as well as experimentally for many years, the spectrum of the lightest resonances in QCD is still not understood from first principles. The only known way to extract nonperturbative quantities from QCD is the use of lattice QCD. However, current calculations are typically still done for relatively high quark masses (see, e.g., Refs. [1, 2]). Thus, in order to make contact with experiment, appropriate extrapolation formulas need to be derived. This is typically done by using chiral perturbation theory (ChPT), the low energy effective theory of QCD [3, 4]. ChPT predictions are model independent and, in particular, provide, as an expansion, the dependence of observables on the quark masses (or equivalently the pion mass). The aim of this Letter is to predict the quark-mass dependence of the  $\sigma$  and the  $\rho$  mesons from basic principles, namely, using ChPT to next-to-leading order (NLO), unitarity, and analyticity in the form of dispersion theory using the inverse amplitude method (IAM) [5]. It is obtained from a subtracted dispersion relation of the inverse amplitude, whose imaginary part in the elastic region is known exactly from unitarity. All dependences on QCD parameters appear through the ChPT expansion, which is used to calculate the low energy subtraction points and the left cut. Hence, up to a given order in ChPT, the approach has no model dependences. For this work, we will use the NLO  $SU(2)$  elastic IAM whose parameters are fitted to  $\pi\pi$  scattering data, and therefore, our results are *model independent only up to NLO ChPT*.

The use of dispersive methods also allows for a straightforward extension to the second Riemann sheet of the complex plane where poles associated to resonances occur. In this way both  $\sigma$  and  $\rho$  poles appear naturally without any further assumptions and have the correct dependence on QCD parameters up to the order of the ChPT expansion used in the IAM. For instance, from a study of the leading  $1/N_c$  behavior of the amplitudes it was possible to conclude that the  $\rho$  is mostly of  $\bar{q}q$  nature whereas the  $\sigma$  is predominantly non- $\bar{q}q$  [6].

In this Letter, we study how this different structure encoded in the ChPT parameters gets reflected in the quark mass dependence. As we will see, also with respect

to the quark-mass dependence, the  $\rho$  behaves differently than the  $\sigma$ . We will show that for sufficiently large quark (pion) masses, both states become stable poles on the physical sheet; however, this limit is approached very differently, only in part due to their different quantum numbers.

Another motivation for this study is the Anthropic Principle [7], i.e., the need for a subtle fine tuning of various parameters of the Standard Model. In order to allow for an efficient triple  $\alpha$  process, necessary for the production of carbon, a  $NN$  interaction within 2 % of the known strength is necessary. Since the  $\sigma$  meson plays a central role in the  $NN$  interaction, this leads to bounds for the sigma mass and, correspondingly, for the quark masses [8]. This issue is particularly exciting, if the fundamental constants were time dependent, as claimed in Ref. [9]. In this context the quark mass dependence of the  $\sigma$  was studied in Ref. [10].

We are interested in  $\pi\pi$  elastic amplitudes projected on partial waves  $t_{IJ}$  of definite isospin  $I$  and total angular momentum  $J$ . For simplicity, we will drop the  $IJ$  labels. Note that the  $\sigma$  ( $\rho$ ) resonance appears as a pole in the second Riemann sheet of the partial wave  $(I, J) = (0, 0)$   $((1, 1))$ . Elastic unitarity implies:

$$\text{Im } t(s) = \sigma(s) |t(s)|^2, \quad \Rightarrow \quad \text{Im } [t(s)^{-1}] = -\sigma(s), \quad (1)$$

where  $s$  is the usual Mandelstamm variable for the total energy,  $\sigma(s) = p/(2\sqrt{s})$  and  $p$  is the center of mass momentum. Consequently, the imaginary part of the elastic inverse amplitude is known exactly.

In this Letter, we focus on the two lightest resonances of QCD, the  $\rho(770)$  and the  $f_0(600)$ . It is therefore enough to work with the two lightest quark flavors  $u, d$  in the isospin limit of an equal mass  $\hat{m} = (m_u + m_d)/2$ . The pion mass is given by an expansion  $m_\pi^2 \sim \hat{m} + \dots$  [4]. Therefore, studying the quark mass dependence is equivalent to studying the  $m_\pi$  dependence.

ChPT amplitudes are obtained as a series expansion  $t = t_2 + t_4 + \dots$  with  $t_k = O(p^k)$ , where  $p$  stands generically either for pion momenta or masses. The leading order,  $t_2$ , which is obtained at tree level from the  $O(p^2)$  Lagrangian, is just a polynomial fixed by chiral symme-

try in terms of the pion mass and its decay constant  $f_\pi$ . The NLO term  $t_4$  has both one-loop contributions from the  $O(p^2)$  Lagrangian and tree level contributions from the  $O(p^4)$  Lagrangian. The latter depend on a set of low energy constants (LEC), denoted by  $l_i$ , that absorb the one-loop divergences through renormalization. Since these constants are the coefficients of the energy and mass expansion *the  $l_i$  have no quark mass dependence*. In contrast,  $f_\pi$  gets renormalized at NLO and thus depends explicitly on the pion mass.

The ChPT series, being an expansion, satisfies unitarity, Eq.(1), just perturbatively:

$$\text{Im } t_4(s) = \sigma(s)|t_2(s)|^2, \quad \Rightarrow \quad \text{Im } \frac{t_4(s)}{t_2(s)^2} = \sigma(s), \quad (2)$$

and cannot generate poles. Therefore the resonance region lies beyond the reach of standard ChPT. However, it can be reached by combining ChPT with dispersion theory either for the amplitude [11] or the inverse amplitude through the IAM [12, 13, 14].

**3.** The IAM uses the ChPT series to generate resonances in meson-meson scattering. In the elastic case, the IAM follows from dispersion theory [12, 13] due to the fact that  $t$  and  $1/t$  have an almost identical analytic structure: both have a “physical cut” from threshold to  $\infty$  and a “left cut” from  $-\infty$  to  $s = 0$ . In addition, the inverse amplitude may have a pole whenever the amplitude vanishes. For the  $\rho$ -channel, this happens at threshold to all orders, but for scalar waves it occurs at the so-called Adler zero  $s_A$ , that lies on the real axis below threshold, thus within the ChPT region of applicability. Its position can be obtained from the ChPT series, i.e.,  $s_A = s_2 + s_4 + \dots$ , where  $t_2$  vanishes at  $s_2$ ,  $t_2 + t_4$  at  $s_2 + s_4$ , etc... Thus we can write a dispersion relation for the inverse amplitude,

$$\frac{1}{t(s)} = \frac{s - s_A}{\pi} \int_{RC} dz \frac{\text{Im } 1/t(z)}{(z - s_A)(z - s)} + LC_{\frac{1}{t}} + PC_{\frac{1}{t}}, \quad (3)$$

where “LC” stands for a similar integral over the left cut. To ensure convergence we have made a subtraction precisely at  $s_A$ . Since  $t_2$  is real on the real axis, we can similarly write

$$\frac{t_4(s)}{t_2(s)^2} = \frac{s - s_2}{\pi} \int_{RC} dz \frac{\text{Im } t_4(z)/t_2(z)^2}{(z - s_2)(z - s)} + LC_{\frac{t_4}{t_2^2}} + PC_{\frac{t_4}{t_2^2}}. \quad (4)$$

We can now use unitarity, Eqs.(1) and (2), to find that the integrand numerators are *exactly opposite*. Since the  $LC$  integral is weighted at low energies, using NLO ChPT, we also find  $LC(1/t) \simeq -LC(t_4/t_2^2)$ . Consequently, crossing symmetry is satisfied just up to NLO. In the above relations,  $PC_{1/t}$  and  $PC_{t_4/t_2^2}$  stand for the contributions of a double and triple pole respectively, which can be easily calculated within ChPT. Their contribution is only relevant around the Adler zero, where they diverge. Finally, we can use ChPT to approximate

$(s - s_A)/(z - s_A) \simeq (s - s_2)/(z - s_2)$ . Altogether, we find

$$t^{mIAM}(s) = \frac{t_2^2(s)}{t_2(s) - t_4(s) + A^{mIAM}(s)}, \quad (5)$$

$$A^{mIAM}(s) = t_4(s_2) - \frac{(s_2 - s_A)(s - s_2)[t_2'(s_2) - t_4'(s_2)]}{s - s_A}.$$

The usual IAM is recovered for  $A^{mIAM} \equiv 0$ , which holds exactly for all partial waves but the scalar ones. In the original IAM dispersive derivation [12, 13]  $A^{mIAM}$  was neglected, since it formally yields a NNLO contribution. However, due to neglecting  $A^{mIAM}$ , the IAM has a spurious pole close to its Adler zero, which is only correct to LO ChPT. As we will see, for large  $m_\pi$  the  $\sigma$  pole splits into two virtual poles below threshold, one of them moving towards zero and eventually approaching the spurious pole of the IAM. Thus, although the Adler zero ( $\simeq m_\pi/\sqrt{2}$ ) is very deep in the subthreshold region, we used the modified IAM (mIAM) [5, 15], which has no spurious pole, and reproduces the Adler zero up to NLO. Switching from the IAM to the mIAM influences only the mentioned second  $\sigma$  pole, and only when it is very close to the spurious pole (this occurs when  $M_\sigma \leq 1.5m_\pi$ ). Besides this, the IAM and mIAM results are essentially the same. For subtractions made at different low energy points,  $A^{mIAM}$  acquires additional NNLO terms, but their effect is negligible [5].

Therefore, *up to a given order in ChPT*, the elastic (m)IAM is built in a model independent way from the first principles of unitarity and analyticity in the form of a dispersion relation. The ChPT series is used only on the Adler zeros and the left hand cut which is heavily weighted at low energies, thus well within its region of applicability. It is a dispersion integral for the inverse amplitude that allows us to study the resonance region.

Although remarkably simple, the (m)IAM amplitudes satisfy elastic unitarity, Eq.(1), exactly, and provide a very good description of meson-meson scattering data simultaneously in the resonance and low energy regions [12, 13, 14]. Furthermore, the IAM generates the poles in the second Riemann sheet associated to the resonances, namely  $\sigma$  and  $\rho$ . This description is obtained with values of the LEC compatible with those of standard ChPT [13, 14]. Actually, the ChPT series up to NLO is recovered when Eq. (5) is reexpanded at low energies. Thus, after a fit to data we can modify  $m_\pi$  and follow the poles associated to  $\rho$  and  $\sigma$  on the second sheet.

As long as they fall within their uncertainties, the precise values of the LECs  $l_3^r$  and  $l_4^r$  are not very relevant for this study. We take from [4]  $10^3 l_3^r = 0.8 \pm 3.8$ ,  $10^3 l_4^r = 6.2 \pm 5.7$ . Then we fit the mIAM to data up to the resonance region and find  $10^3 l_1^r = -3.7 \pm 0.2$ ,  $10^3 l_2^r = 5.0 \pm 0.4$ . All these LEC are evaluated at  $\mu = 0.77 \text{ GeV}$ .

The values of  $m_\pi$  considered should fall within the ChPT range of applicability and allow for some elastic  $\pi\pi$  regime to exist below  $K\bar{K}$  threshold. Both criteria are satisfied, if  $m_\pi \leq 0.5 \text{ GeV}$ , since we know SU(3) ChPT still works fairly well with such a kaon mass, and because

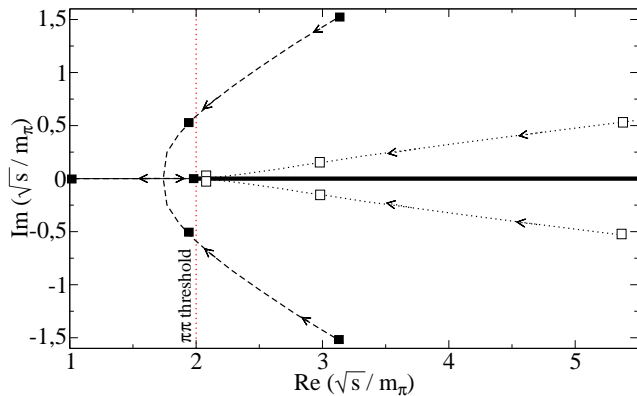


FIG. 1: Movement of the  $\sigma$  (dashed lines) and  $\rho$  (dotted lines) poles for increasing pion masses (direction indicated by the arrows) on the second sheet. The filled (open) boxes denote the pole positions for the  $\sigma$  ( $\rho$ ) at pion masses  $m_\pi = 1, 2$ , and  $3 \times m_\pi^{\text{phys}}$ , respectively. Note, for  $m_\pi = 3m_\pi^{\text{phys}}$  three poles accumulate in the plot very near the  $\pi\pi$  threshold.

for  $m_\pi \simeq 0.5$  GeV, the kaon mass becomes  $\simeq 0.6$  GeV, leaving a 0.2 GeV gap to the two-kaon threshold. For larger values of  $m_\pi$  a coupled-channel IAM is needed, which is feasible, but lies beyond our present scope, and lacks a dispersive derivation.

Fig. 1 shows, in the second Riemann sheet, the  $\rho$  and  $\sigma$  poles for the physical  $m_\pi$ , and how they move as  $m_\pi$  increases. Note that, associated to each resonance, there are two conjugate poles that move symmetrically on each side of the real axis. In order to see more clearly that all poles move closer to the two-pion threshold, which is also increasing, all quantities are given in units of  $m_\pi$  so that the two-pion threshold is fixed at  $\sqrt{s} = 2$ . Let us recall that, for narrow resonances, their mass  $M$  and width  $\Gamma$  are related to the pole position in the lower half plane as  $\sqrt{s_{\text{pole}}} \simeq M - i\Gamma/2$  and customarily this notation is also kept for broader resonances. Hence, both  $\Gamma_\sigma$  and  $\Gamma_\rho$  decrease for increasing  $m_\pi$ . In particular,  $\Gamma_\rho$  vanishes exactly at threshold where one pole jumps into the first sheet, thus becoming a traditional stable state, while its partner remains on the second sheet practically at the very same position as the one in the first. In contrast, when  $M_\sigma$  reaches the two-pion threshold, its poles remain on the second sheet with a non-zero imaginary part before they meet on the real axis and become virtual states. As  $m_\pi$  increases further, one of those virtual states moves towards threshold and jumps onto the first sheet, whereas the other one remains in the second sheet. Such an analytic structure, with two very asymmetric poles in different sheets of an angular momentum zero partial wave, is a strong indication for a prominent molecular component [16, 17]. Differences between P-wave and S-wave pole movements were also found within quark models [18], the latter also showing two second sheet poles on the real axis below threshold.

In the upper panel of Fig. 2 we show the  $m_\pi$  depen-

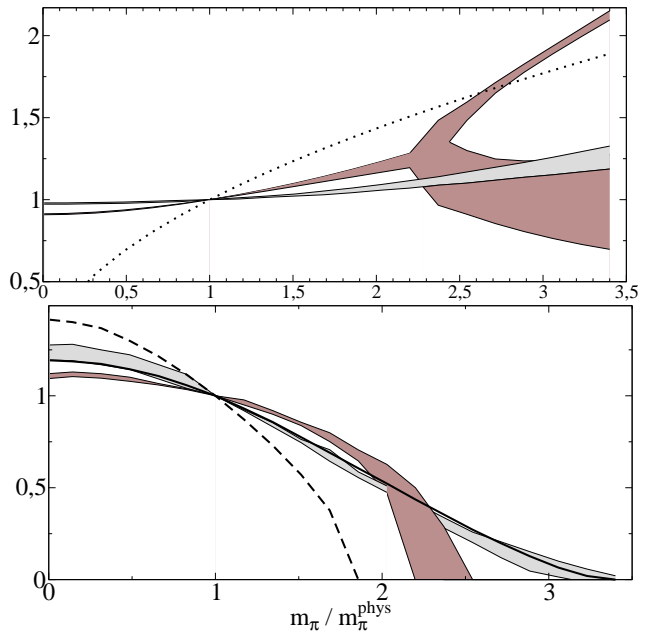


FIG. 2:  $m_\pi$  dependence of resonance masses (upper panel) and widths (lower panel) in units of the physical values. In both panels the dark (light) band shows the results for the  $\sigma$  ( $\rho$ ). The width of the bands reflects the uncertainties induced from the uncertainties in the LEC. The dotted line shows the  $\sigma$  mass dependence estimated in Ref. [8]. The dashed (continuous) line shows the  $m_\pi$  dependence of the  $\sigma$  ( $\rho$ ) width from the change of phase space only, assuming a constant coupling of the resonance to  $\pi\pi$ .

dence of  $M_\sigma$  and  $M_\rho$  normalized to their physical values. The bands cover the LEC uncertainties. Note, that significant, additional uncertainties may emerge at the two loop level for pion masses larger than 0.3 GeV — see, e.g., Ref. [19]. We see that both masses grow with increasing  $m_\pi$ , but the rise of  $M_\sigma$  is stronger than that of  $M_\rho$ , and again we see that around  $m_\pi \simeq 0.33$  GeV the  $\sigma$  state splits into two virtual states with different behavior. The upper branch moves closer to threshold and thus has the biggest influence in the physical region, eventually jumping to the first Riemann sheet. Note that the  $m_\pi$  dependence of  $M_\sigma$  is much softer than that suggested in the model of [8], shown as the dotted line, which in addition does not show the virtual pole splitting.

In the lower panel of Fig. 2 we show the  $m_\pi$  dependence of  $\Gamma_\sigma$  and  $\Gamma_\rho$  normalized to their physical values. The decrease in  $\Gamma_\rho$  is largely kinematical, following remarkably well the expected reduction from phase space as  $m_\pi$  and  $M_\rho$  increase. In other words, the effective coupling of the  $\rho$  to  $\pi\pi$  is almost  $m_\pi$  independent. This was assumed in the analysis of Ref. [20]; however, so far this assumption has not been supported by theory. In sharp contrast to this behavior is the one of  $\Gamma_\sigma$ . This suggests a strong pion mass dependence of the  $\sigma$  coupling to two pions, necessarily present for molecular states [17, 21].

Fig. 3 is a comparison of our results for the  $m_\pi$  de-

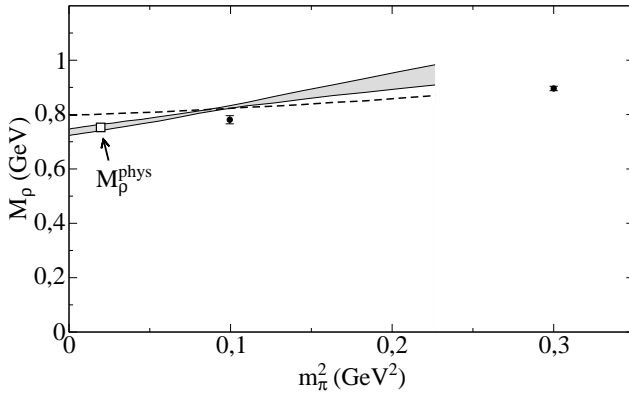


FIG. 3: The grey band shows the  $m_\pi$  dependence of  $\rho$  pole mass from the IAM versus recent lattice results from [1]. The dashed line is the IAM result for  $N_c = 10$ .

pendence of  $M_\rho$  with some recent unquenched lattice results [1], which deserves several words of caution. In particular, our approach only ensures the  $m_\pi$  dependence contained in the NLO ChPT series — it is, e.g., lacking terms of order  $m_\pi^2 p^4$  and higher. In addition,  $M_\rho$  is the ‘pole mass’ which, particularly for physical values, is deep in the complex plane, while, due to the finite lattice volume, the minimum energy with which pions are produced on the lattice is larger than the resulting  $M_\rho$ . In our formalism, we can mimic a narrow  $\rho$  by increasing the number of colors [6]. We also show the result of rescaling the IAM ChPT amplitudes from  $N_c = 3$  to  $N_c = 10$ , which effectively reduces  $\Gamma_\rho$  by a factor of  $3/10$ . Although this narrowing effect is not exactly the same as that on the lattice — it is more like quenching the lattice results, since the large  $N_c$  expansion actually sup-

presses quark loops — it is encouraging that making the  $\rho$  artificially narrower yields a better agreement with the quark-mass dependence of the lattice data. With these caveats in mind our results are in qualitative agreement with the lattice results. Following Ref. [22] one may write  $M_\rho = M_\rho^0 + c_1 m_\pi^2 + O(m_\pi^3)$ , where the  $c_i$  parameters are expected to be of order one and  $0.65 \text{ GeV} \leq M_\rho^0 \leq 0.80 \text{ GeV}$ . This is confirmed by a fit to lattice data [1]. From our approach we predict  $M_\rho^0 = 0.735 \pm 0.0017 \text{ GeV}$ . Furthermore, the IAM reproduces  $M_\rho$  at the physical value of  $m_\pi$ , where higher orders in the  $\rho$  mass formula are  $\simeq 15\%$  [22]. Within that uncertainty, we thus get the prediction  $c_1 = 0.90 \pm 0.11 \pm 0.13 \text{ GeV}^{-1}$ . Although the quark-mass dependence of our calculation is steeper than that of Ref. [1], the extracted values are still consistent with the expectations mentioned above — again we remind the reader that the  $m_\pi$  dependence included is correct only to NLO in ChPT.

To summarize, we presented a prediction for the quark mass dependence of the lightest resonances in QCD, namely the  $\rho$  and the  $\sigma$  meson based on chiral perturbation theory at next-to-leading order together with the inverse amplitude method. We showed that the mass of the  $\rho$  has a very smooth  $m_\pi$  dependence and its coupling to  $\pi\pi$  is almost quark-mass independent — in Ref. [20], this was only assumed without further evidence. The mass of the  $\sigma$ , on the other hand, shows a pronounced non-analyticity when  $m_\pi$  is varied. In addition, its effective coupling to  $\pi\pi$  is strongly  $m_\pi$  dependent. This is interpreted as additional evidence for a significant molecular admixture in the sigma, consistent with previous analyses, and will be important for future chiral extrapolations of lattice data for  $s$ -wave resonances.

We thank G. Colangelo, S. Dür, V.V. Flambaum, U.-G. Meißner and A. Rusetsky for their useful comments.

- 
- [1] S. Aoki *et al.*, Phys. Rev. D **60**, 114508 (1999).
  - [2] K. F. Liu, Prog. Theor. Phys. Suppl. **168**, 160 (2007); C. McNeile and C. Michael, Phys. Rev. D **74** (2006) 014508. M. G. Alford and R. L. Jaffe, Nucl. Phys. B **578**, 367 (2000). T. Kunihiro, et al., Phys. Rev. D **70**, 034504 (2004).
  - [3] S. Weinberg, Physica **A96** (1979) 327.
  - [4] J. Gasser and H. Leutwyler, Annals Phys. **158** (1984) 142; Nucl. Phys. B **250** (1985) 465.
  - [5] A. G. Nicola et al., arXiv:0712.2763 [hep-ph].
  - [6] J. R. Peláez and G. Rios, Phys. Rev. Lett. **97** (2006) 242002. J. R. Peláez, Phys. Rev. Lett. **92** (2004) 102001
  - [7] C. J. Hogan, Rev. Mod. Phys. **72**, 1149 (2000) H. Oberhummer et al., Science **289**, 88 (2000) T. Damour and J. F. Donoghue, arXiv:0712.2968 [hep-ph].
  - [8] T. E. Jeltima and M. Sher, Phys. Rev. D **61** (2000) 017301
  - [9] J. K. Webb et al., Phys. Rev. Lett. **82** (1999) 884.
  - [10] V. V. Flambaum and E. V. Shuryak, Phys. Rev. D **65**, 103503 (2002).
  - [11] I. Caprini et al., Phys. Rev. Lett. **96** (2006) 132001
  - [12] T. N. Truong, Phys. Rev. Lett. **61** (1988) 2526. Phys. Rev. Lett. **67**, (1991) 2260; A. Dobado et al., Phys. Lett. **B235** (1990) 134.
  - [13] A. Dobado and J. R. Peláez, Phys. Rev. D **47** (1993) 4883; Phys. Rev. D **56** (1997) 3057.
  - [14] F. Guerrero and J. A. Oller, Nucl. Phys. B **537** (1999) 459 [Erratum-ibid. B **602** (2001) 641]. J. R. Peláez, Mod. Phys. Lett. A **19**, 2879 (2004) A. Gómez Nicola and J. R. Peláez, Phys. Rev. D **65** (2002) 054009 and AIP Conf. Proc. **660** (2003) 102.
  - [15] D. Fernandez-Fraile et al., Phys. Rev. D **76**, 085020 (2007).
  - [16] D. Morgan, Nucl. Phys. A **543** (1992) 632; D. Morgan and M. R. Pennington, Phys. Rev. D **48** (1993) 1185.
  - [17] V. Baru et al., Phys. Lett. B **586** (2004) 53.
  - [18] E. van Beveren et al., AIP Conf. Proc. **660**, 353 (2003); Phys. Rev. D **74**, 037501 (2006).
  - [19] G. Colangelo and S. Dür, Eur. Phys. J. C **33** (2004) 543.
  - [20] S. Aoki et al., Phys. Rev. D **76** (2007) 094506.
  - [21] S. Weinberg, Phys. Rev. **130**, 776 (1963); Y. Kalashnikova et al., Eur. Phys. J. A **24** (2005) 437.
  - [22] P. C. Bruns and U.-G. Meißner, Eur. Phys. J. C **40**, 97 (2005).